

# **Triphenylamine/benzothiadiazole-based Compounds for Non-doped Orange and Red Fluorescent OLEDs with High Efficiencies and Low Efficiency Roll-off**

Zhang Di <sup>a</sup>, Yang Tingting <sup>b</sup>, Xu Huixia <sup>a\*</sup>, Miao Yanqin <sup>a\*</sup>, Chen Runfeng <sup>c</sup>, Shinar Ruth <sup>d</sup>, Shinar Joseph <sup>e</sup>, Wang Hua <sup>a</sup>, Xu Bingshe <sup>a</sup>, Yu Junsheng <sup>f</sup>

<sup>a</sup> *Key Laboratory of Interface Science and Engineering in Advanced Materials, Ministry of Education, Taiyuan University of Technology, Taiyuan 030024, China.*

<sup>b</sup> *Shanxi Province Key Laboratory of Microstructure Functional Materials Institute of Solid State Physical, School of Physics and Electronic Science, Shanxi Datong University, Datong, 037009, China*

<sup>c</sup> *Key Laboratory for Organic Electronics and Information Displays & Institute of Advanced Materials, Nanjing University of Posts & Telecommunications, Nanjing 210023, China*

<sup>d</sup> *Microelectronics Research Center and Electrical & Computer Engineering Department, Iowa State University, Ames, IA 50011, USA.*

<sup>e</sup> *Ames Laboratory, USDOE and Physics & Astronomy Department, Iowa State University, Ames, IA 50011, USA.*

<sup>f</sup> *State Key Laboratory of Electronic Thin Films and Integrated Devices, School of Optoelectronic Science and Engineering, University of Electronic Science and Technology of China (UESTC), Chengdu, 610054, PR China*

**Supporting information**

**General Information**

All reagents and solvents used for the synthesis and characterization were purchased from commercial companies and without further purification.  $^1\text{H-NMR}$  and  $^{13}\text{C-NMR}$  spectra were measured with a Switzerland Bruker DR×600 at 600 and 151 MHz using tetramethylsilane (TMS) as the internal standard. The time-of-flight (MALDI-TOF) mass spectra were collected on a Bruker Daltonics. C, H and N microanalysis were carried out with an Elemental Vario EL elemental analyzer. UV-Vis spectra were recorded using a HTIACH U-3900 Spectrometer. The molar absorption coefficient was calculated according to Beer-Lambert Law:

$$A = \varepsilon cl \quad (1)$$

Where  $A$  is the absorbance,  $\varepsilon$  the molar absorption coefficient,  $c$  the the concentration (mol/L) and  $l$  the optical path length, which corresponds to the path length of quartz cells. The  $\varepsilon$  can be calculated for a tested sample at any given absorption wavelength. Therefore, the radiative decay constant  $k_r$  can be estimated from  $\varepsilon$  at the longest absorption maximum [1]:

$$k_r = \varepsilon_{max} \times 10^4 \quad (2)$$

Where  $\varepsilon_{max}$  is the molar absorption coefficient at the longest absorption maximum.

Photoluminescence (PL) spectra were recorded with a HORIBA FluoroMax-4 spectrometer. The absolute fluorescence quantum yields of the solids were measured on Edinburgh Instrument FLS980 using an integrating sphere. The transient photoluminescence decay measurement was carried out using an Edinburgh Instrument FLS980 spectrometer equipped with an EPL-375 picosecond pulsed diode laser. Thermal gravimetric analysis was performed on a Netzsch TG 209F3 under dry nitrogen atmosphere, heating from room temperature to 800 °C at a rate of 10 °C/min. Differential scanning calorimetry (DSC) was measured on DSC Q2000 at a heating rate of 10°C/min from 20 to 350°C, then cooling down to room temperature rapidly, and heating up to 350°C at a rate of 10°C/min again.

## Electrochemical Measurement

The electrochemical properties were obtained via cyclic voltammetry (CV) measurement by using a CHI 660E voltammetry analyzer. Tetrabutylammoniumhexafluorophosphate (TBAPF<sub>6</sub>) in anhydrous dichloromethane (0.1 M) was used as the electrolyte. A platinum wire was used as the working electrode. A platinum electrode was the counter and a calomel electrode was the reference with ferrocenium-ferrocene (Fc<sup>+</sup>/Fc) as the internal standard. The HOMO/LUMO levels are calculated according to the following formalism:

$$E_{HOMO} = -4.8 - e(E_c^{ox} - E_f^{ox})V \quad (3)$$

where  $E_c^{ox}$  is the first oxidation peaks measured from CV curves and  $E_f^{ox}$  is the oxidation peak of ferrocene. The lowest unoccupied molecular orbital level ( $E_{LUMO}$ ) was calculated from  $E_{LUMO} = E_{HOMO} + E_g$ , and  $E_g$  was estimated from the intersection of absorption and emission spectra.

## Computational details

Theoretical simulations were performed using the Gaussian 03 package. Geometry optimization was performed by density functional theory (DFT) in B3LYP/6-31 G(d) basis sets [2, 3].

## OLED fabrication and characterization

OLEDs with area of  $3 \times 3$  mm<sup>2</sup> were fabricated by thermal vacuum deposition onto indium tin oxide (ITO) glass substrate, which was cleaned with deionized water, acetone, and ethanol, in that order. The EL spectra and CIE coordinates were recorded by PR-655 spectrophotometer. The OLEDs' current density-voltage-luminance ( $J$ - $V$ - $L$ ) characteristics were measured by a computer-controlled Keithley 2400 source meter integrated with a BM-70A luminance meter. The EQE was calculated from the  $J$ - $V$ - $L$  curves and spectra data. All devices were characterized without

encapsulation in ambient atmosphere at room temperature.

The doped devices' structure was (ITO) /MoO<sub>3</sub> (3 nm)/NPB (30 nm)/TCTA (10 nm)/CBP: 30 wt% emitters (20 nm)/BePP<sub>2</sub> (50 nm)/LiF (1 nm)/Al (100 nm). ITO and Al are used as the anode and cathode, respectively; MoO<sub>3</sub> and LiF acted as the hole and electron injection layers, respectively; NPB (N, N'-di(1-naphthyl)-N, N'-diphenyl-(1,1'-biphenyl)-4,4'-diamine) and TCTA (tris(4-carazoyl-9-ylphenyl)amine) are served as hole-transport layer and electron blocking layer, respectively, and Bepp<sub>2</sub> (pp = 2-(2-hydroxyphenyl)pyridine) was used as the electron-transport layer.

The non-doped devices were of the configuration: ITO /MoO<sub>3</sub> (3 nm)/NPB (30 nm)/TCTA (10 nm)/emitter (20 nm)/BePP<sub>2</sub> (50 nm)/LiF (1 nm)/Al (100 nm).

The single carrier devices included hole-only devices (HOD) of ITO/ MoO<sub>3</sub> (3 nm)/ TCTA (10 nm)/emitters (60 nm)/ TCTA (10 nm)/ Al (100 nm) and electron-only devices (EOD) of ITO / TPBI (10 nm) /BePP<sub>2</sub> (60 nm)/ TPBI (10 nm)/ LIF (1 nm)/Al (100 nm).

## Synthesis

Synthesis of 4-(7-(10-(naphthalen-2-yl)anthracen-9-yl)benzo[c][1,2,5]thiadiazol-4-yl) -N,N-diphenylaniline (**TPA-BT-AN-NA**)

(a) Synthesis of 4-(7-bromobenzo[c][1,2,5]thiadiazol-4-yl)-N,N-diphenylaniline (**1**)

A mixture of 4,7-dibromobenzo[c][1,2,5]thiadiazole (1.00 g, 3.40 mmol), (4-(diphenylamino)phenyl)boronic acid (1.18 g, 4.08 mmol), Pd(PPh<sub>3</sub>)<sub>4</sub> (196 mg, 0.17 mmol), K<sub>2</sub>CO<sub>3</sub> (2.35 g, 17.0 mmol), ultra-pure water (8 mL) and 1,2-dimethoxyethane (40 mL) was stirred at 85°C for 12 h under nitrogen. After cooling to room temperature, the mixture was poured into water, extracted with dichloromethane (DCM), and dried over anhydrous MgSO<sub>4</sub>. Following removal of the solvents, the crude product was purified via column chromatography on silica gel using petroleum

ether/DCM (3:1 v/v) as the eluent to give an orange solid (1.19 g, yield 56%). <sup>1</sup>H NMR (600 MHz, CDCl<sub>3</sub>) δ: 7.90 (d, 1H), 7.83- 7.78 (m, 2H), 7.55 (d, 1H), 7.35 -7.27 (m, 4H), 7.19 (ddd, 6H), 7.08 (t, 2H).

(b) Synthesis 4-(7-(10-(naphthalen-2-yl)anthracene-9-yl)benzo[c][1,2,5]thiadiazol-4-yl)-N,N - diphenylaniline (**TBAN**):

**TBAN** was prepared with a similar procedure as that of intermediate material of **1**. The desired product was obtained as a yellow powder (0.6 g, yield: 60%). <sup>1</sup>H NMR (600 MHz, CDCl<sub>3</sub>) δ: 8.11 – 8.08 (m, 1H), 8.07 - 8.01 (m, 3H), 7.95 (dd, 2H), 7.84 (dd, 1H), 7.77 (d, 2H), 7.70 (d, 1H), 7.67 - 7.52 (m, 5H), 7.35 -7.28 (m, 8H), 7.26 - 7.22 (m, 6H), 7.10 (dd, 2H). <sup>13</sup>C NMR (151 MHz, CDCl<sub>3</sub>) δ: 158.64, 156.08, 150.82, 150.01, 140.62, 139.06, 136.24, 135.95, 135.33, 135.00, 134.65, 133.34, 132.63, 131.91, 130.73, 130.45, 129.94, 129.47, 128.91, 128.06, 127.53, 125.94, 125.38. MS (MALDI-TOF): *m/z* calcd calculated: 681.22 [*M*]<sup>+</sup>; found: 681.218. Elemental analysis calculated for C<sub>48</sub>H<sub>31</sub>N<sub>3</sub>S: C, 84.55; H, 4.58; N, 6.16. Found: C, 84.40; H, 4.50; N, 6.12.

(b) Synthesis of 4,4'-(benzo[c][1,2,5]thiadiazole-4,7-diyl)bis(N,N-diphenylaniline) (**TBT**)

**TBT** was prepared with a similar procedure as that of the intermediate material of **1**. The desired product was obtained as orange powder. <sup>1</sup>H NMR (600 MHz, CDCl<sub>3</sub>) δ: 7.90 - 7.87 (m, 4H), 7.75 (s, 2H), 7.31 - 7.28 (m, 8H), 7.23 - 7.17 (m, 12H), 7.08 - 7.05 (m, 4H). <sup>13</sup>C NMR (101 MHz, CDCl<sub>3</sub>) δ: 154.18, 148.00, 147.52, 132.17, 131.03, 129.93, 129.39, 127.46, 124.91, 123.32, 122.97. MS (MALDI-TOF): *m/z* calcd calculated: 622.22 [*M*]<sup>+</sup>; found: 622.21. Elemental analysis calculated for C<sub>42</sub>H<sub>30</sub>N<sub>4</sub>S: C, 81.0; H, 4.86; N, 9.00. Found: C, 79.94; H, 4.80; N, 9.01.

(d) Synthesis of 4-(7-(10-(4-(diphenylamino)phenyl)anthracen-9-yl)benzo[c][1,2,5]thiadiazol-4-yl) -

## N,N-diphenylaniline (**TBAT**)

Intermediate material **2** and target product **TBAT** were prepared using similar procedure as that of intermediate material **1**. The desired product was obtained as a yellow powder. **2**:  $^1\text{H}$  NMR (600 MHz, Acetone)  $\delta$ : 8.66 (dd, 2H), 8.17 (dd, 2H), 7.92 (d, 2H), 7.72 (ddd, 2H), 7.59 (d, 2H), 7.45 - 7.38 (m, 6H), 7.26 - 7.19 (m, 6H), 7.15 (td, 2H). **TBAT**:  $^1\text{H}$  NMR (600 MHz,  $\text{CDCl}_3$ )  $\delta$ : 7.47 - 7.45 (m, 2H), 7.41 - 7.38 (m, 4H), 7.31 - 7.29 (m, 2H), 7.22 - 7.20 (m, 8H), 7.16 - 7.14 (m, 10H), 6.93 - 6.85 (m, 12H).  $^{13}\text{C}$  NMR (151 MHz,  $\text{CDCl}_3$ )  $\delta$ : 159.05, 150.77, 150.44, 135.35, 135.12, 133.25, 133.01, 132.28, 130.37, 129.83, 129.27, 128.38, 127.93, 127.66, 126.32, 126.03, 125.79. MS (MALDI-TOF):  $m/z$  calcd: 798.28 [ $M$ ] $^+$ ; found: 798.28. Elemental analysis calculated for  $\text{C}_{48}\text{H}_{31}\text{N}_3\text{S}$ : C, 84.18; H, 4.79; N, 7.01. Found: C, 84.20; H, 4.09; N, 6.99.

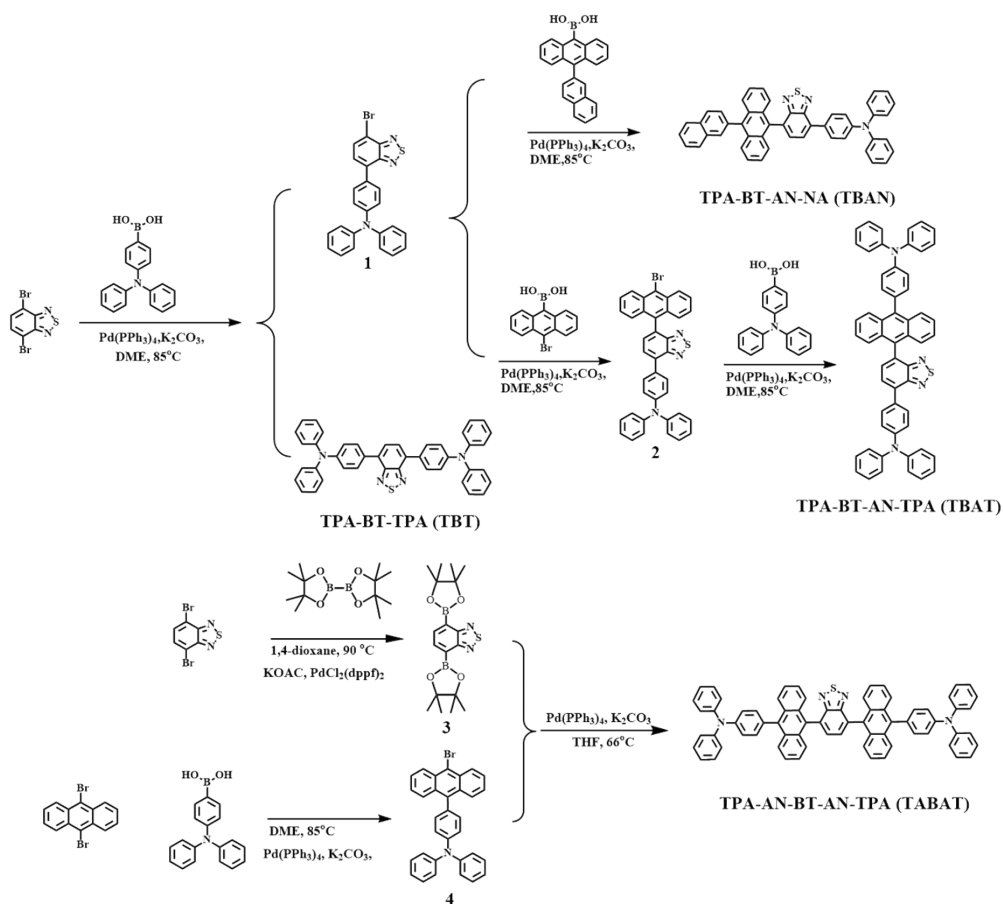
(e) Synthesis of 4,4'-(benzo[*c*][1,2,5]thiadiazole-4,7-diylbis(anthracene-10,9-diyl))bis(N,N-diphenylaniline) (**TABAT**)

### 4,7-bis(4,4,5,5-tetramethyl-1,3,2-dioxaborolan-2-yl)benzo[*c*][1,2,5]thiadiazole (**3**)

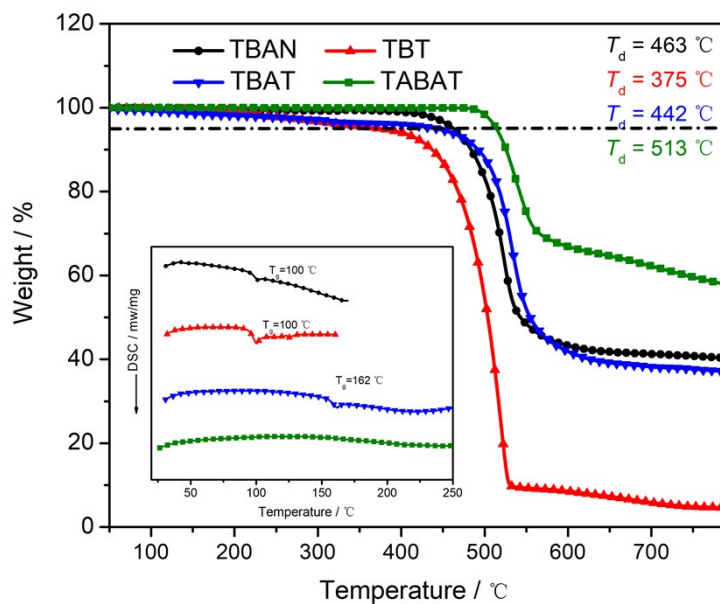
A mixture of 4,7-dibromobenzo[*c*][1,2,5]thiadiazole (3.00 g, 10.2 mmol), 4,4,4',4',5,5,5',5'-octamethyl-2,2'-bi(1,3,2-dioxaborolane) (6.48 g, 25.5 mmol),  $\text{Pd}(\text{dppf})\text{Cl}_2$  (224 g, 0.31 mmol), KOAC (6.01 g, 61.2 mmol), and 1,4-dioxane (50 mL) was stirred at 90°C for 12 h under nitrogen. After cooling to room temperature, the mixture was poured into water, extracted with dichloromethane (DCM), and dried over anhydrous  $\text{MgSO}_4$ . After removal of the solvents, the crude product was purified via column chromatography on silica gel using petroleum ether/DCM (1: 1 v/v) as the eluent to give a yellow solid.  $^1\text{H}$  NMR (400 MHz,  $\text{CDCl}_3$ )  $\delta$ : 8.13 (s, 2H), 1.44 (s, 24H).

Intermediate material **4** and target product **TABAT** were prepared with a similar procedure as that of intermediate material of **1**. **4**:  $^1\text{H}$  NMR (600 MHz, Acetone)  $\delta$ : 8.62-8.57 (m, 2H), 7.85 -7.81 (m, 2H),

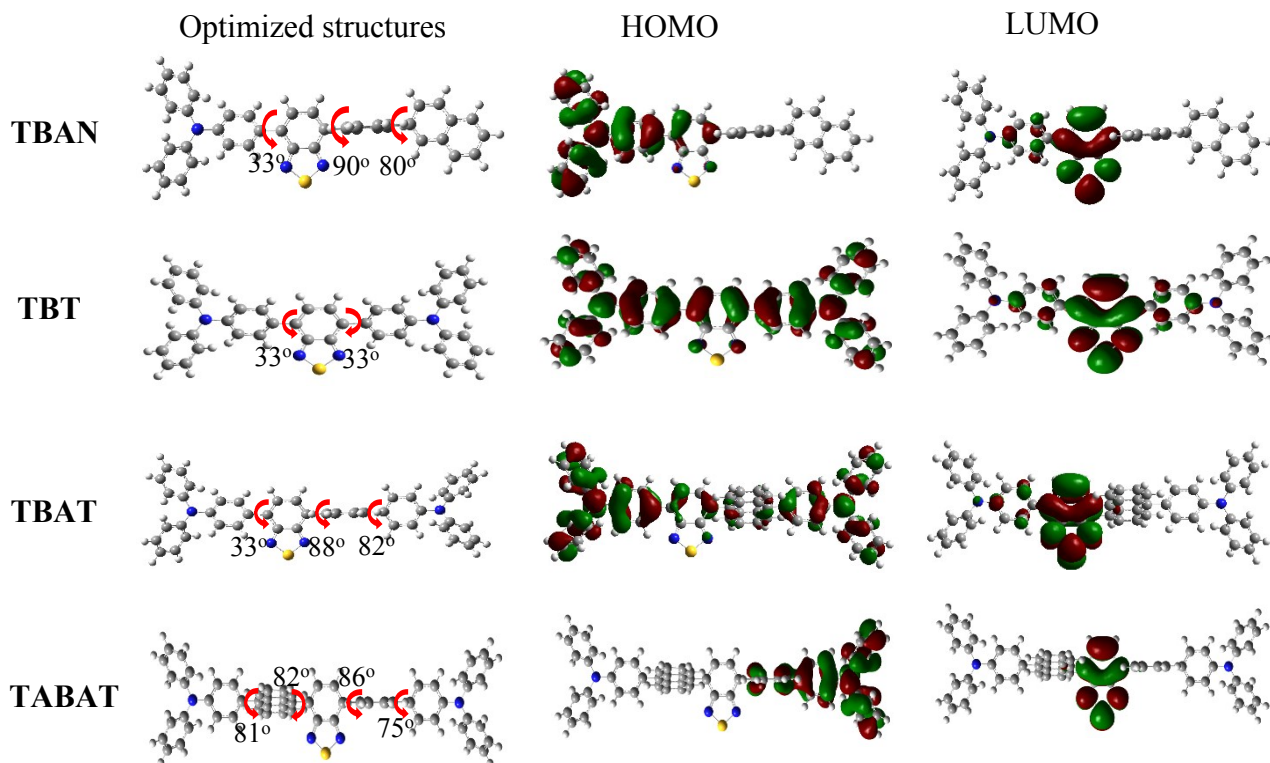
7.71 (ddd, 2H), 7.53 (ddd, 2H), 7.41 -7.37 (m, 4H), 7.36-7.33 (m, 2H), 7.31 - 7.24 (m, 6H), 7.13 (tt, 2H). **TABAT**:  $^1\text{H NMR}$  (600 MHz,  $\text{CDCl}_3$ )  $\delta$ : 8.03 (s, 2H), 7.99 -7.95 (m, 4H), 7.75 - 7.66 (m, 4H), 7.47 - 7.45 (m, 8H), 7.36 (ddd, 16H), 7.31 (d, 8H), 7.11 (t, 4H). **MS** (MALDI-TOF):  $m/z$  calcd calculated: 974.34  $[M]^+$ ; found: 974.35. Elemental analysis calculated for  $\text{C}_{70}\text{H}_{46}\text{N}_4\text{S}$ : C, 86.21; H, 4.75; N, 5.75. Found: C, 87.25; H, 4.75; N, 5.78.



**Scheme S1.** Synthetic procedures and chemical structures of all synthesized molecules



**Fig. S1** TG and DSC curves of TBNA, TBT, TBAT and TABAT



**Fig. S2** Optimized structures, HOMO and LUMO electron density of TBAN, TBT, TBAT and TABAT



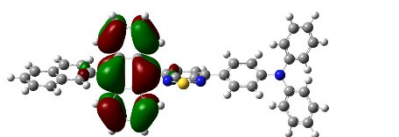
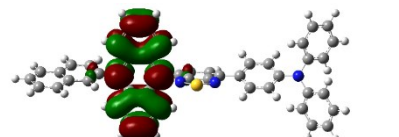
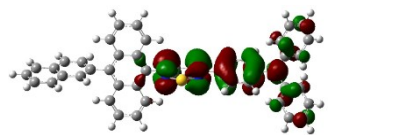
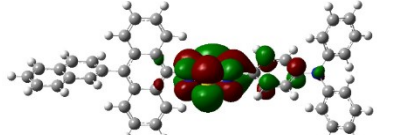
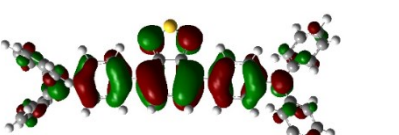
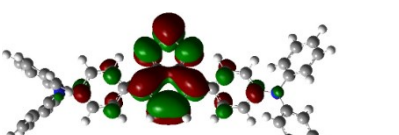
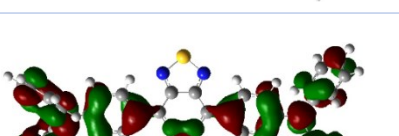
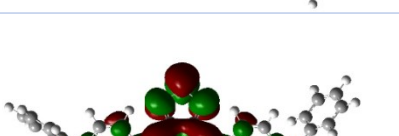

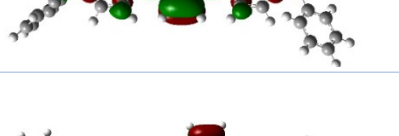
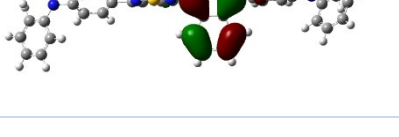
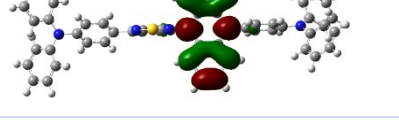
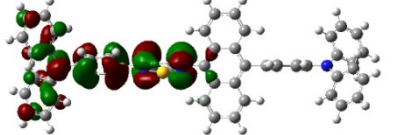

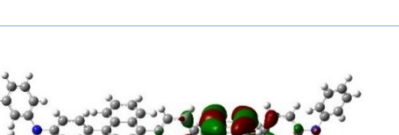
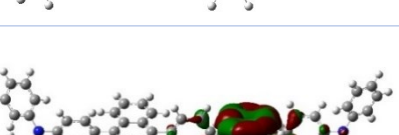
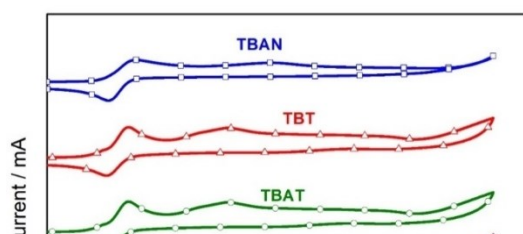
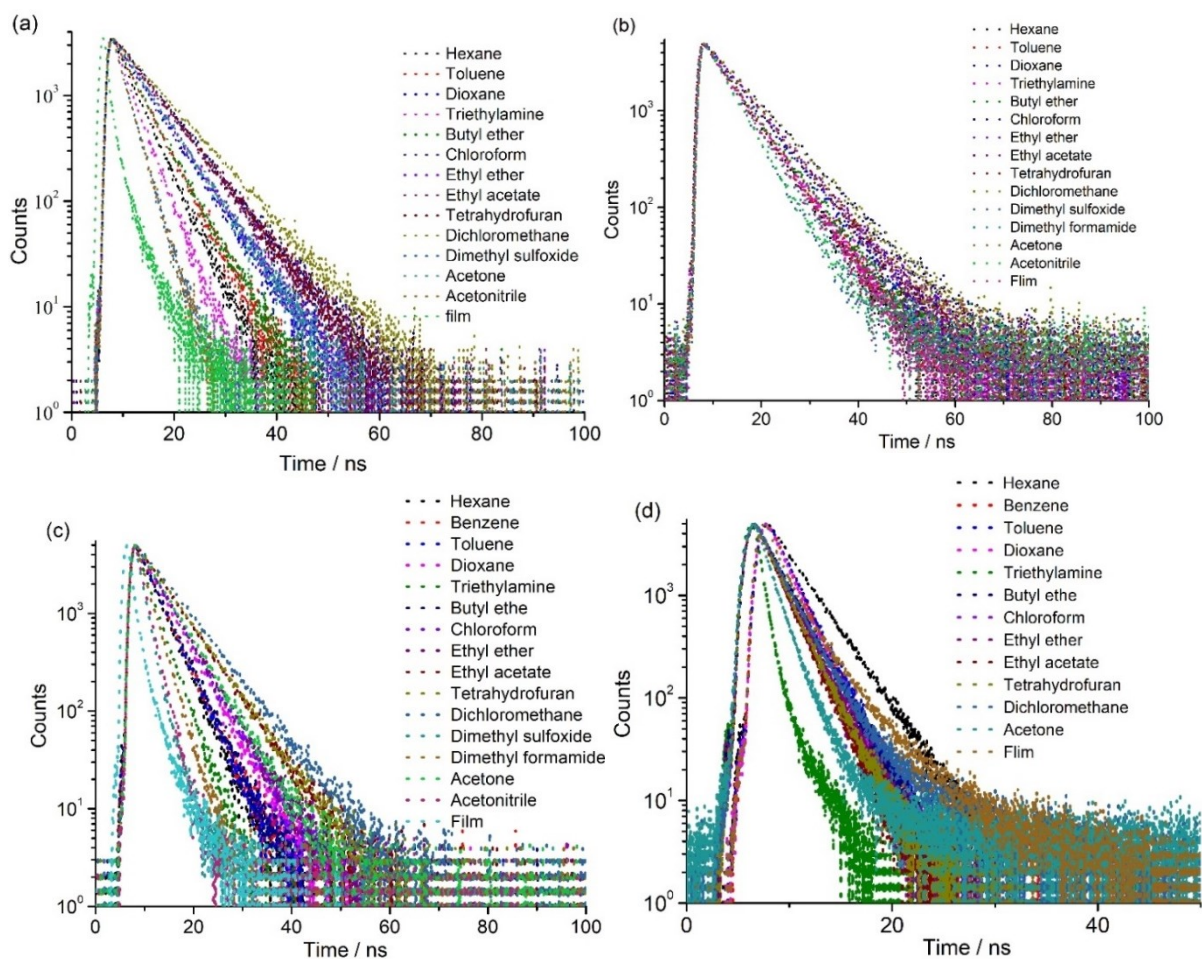
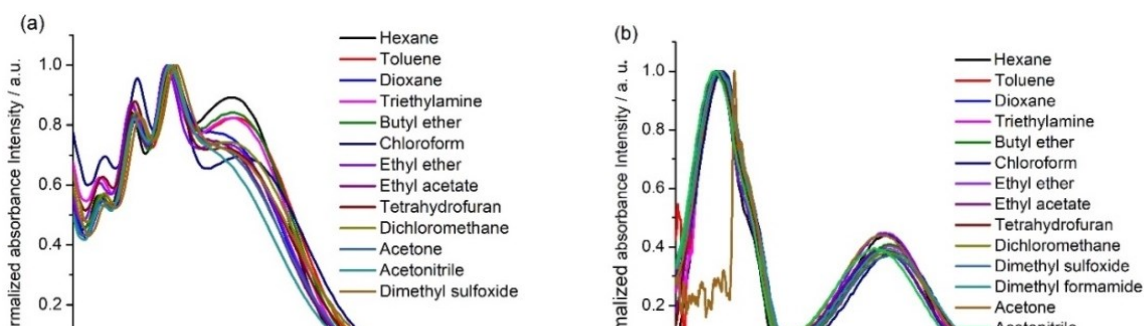
Molecule	State	Hole (HONTO)	Particle (LUNTO)
TBAN	T <sub>1</sub>		
	T <sub>3</sub>		
TBT	T <sub>1</sub>		
	T <sub>3</sub>		
TBAT	T <sub>1</sub>		
	T <sub>3</sub>		
TABAT	T <sub>1</sub>		
	T <sub>3</sub>		

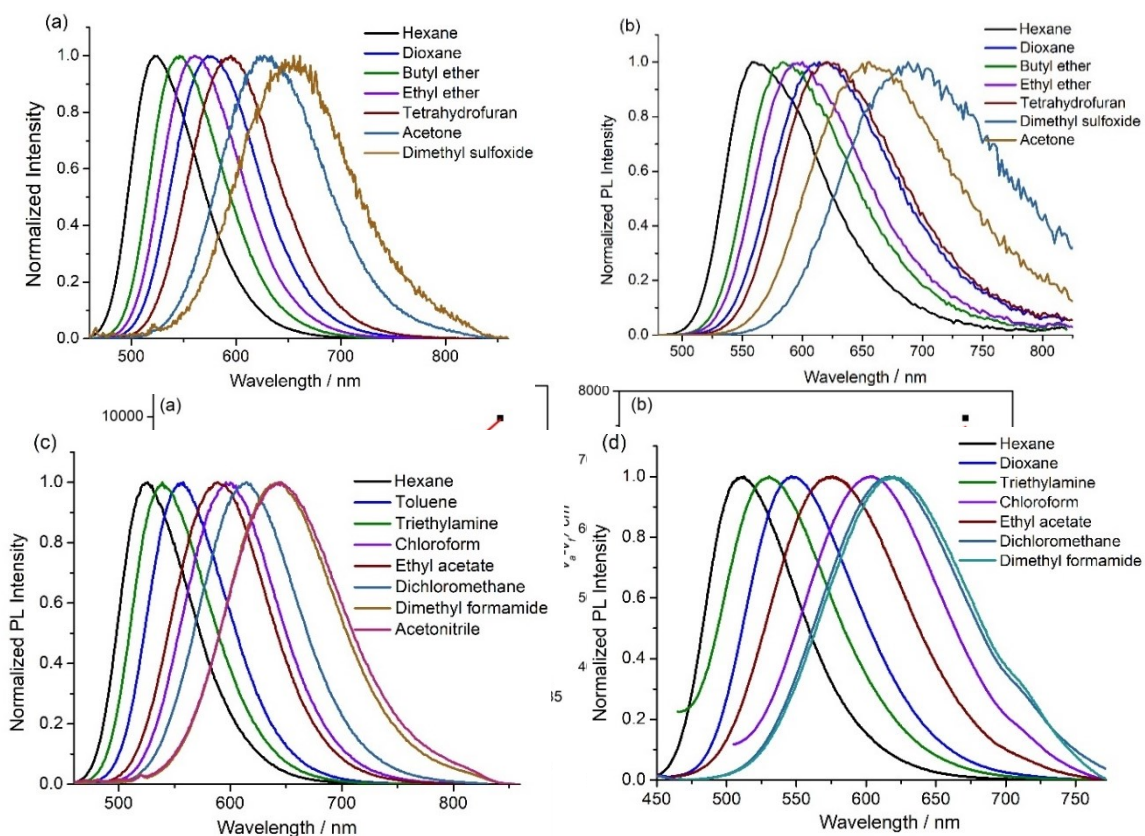
Fig. S3 The natural transition orbitals of all molecules





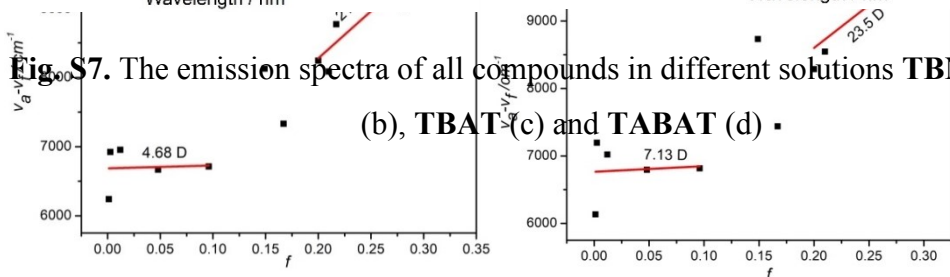
**Fig. S5** Transient PL decay spectra of TBNA (a), TBT (b), TBAT (c), and TABAT (d) in different solvents with increasing polarities and neat film



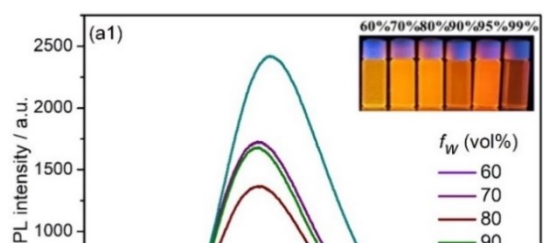
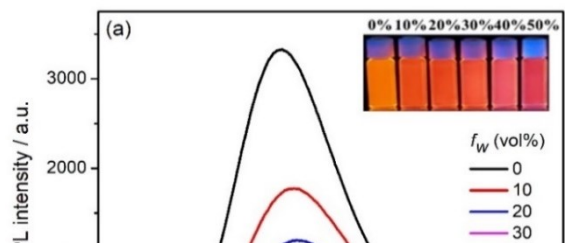


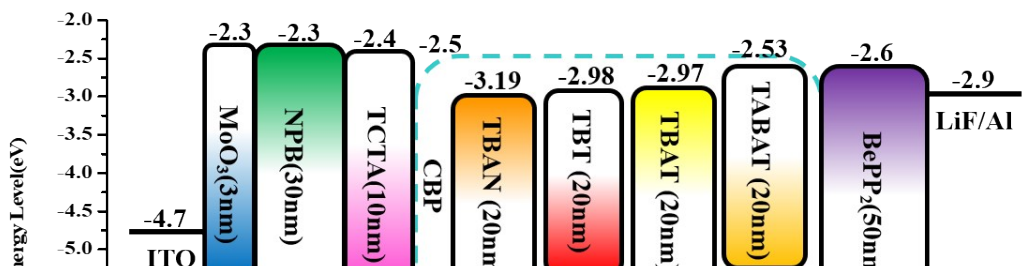
**Fig. S7.** The emission spectra of all compounds in different solutions **TBNA** (a), **TBT**

(b), **TBAT** (c) and **TABAT** (d).



**Fig. S8** Linear correlation of orientation polarization ( $f$ ) of solvent with the Stokes shift for **TBNA** (a), **TBT** (b), **TBAT** (c) and **TABAT** (d)





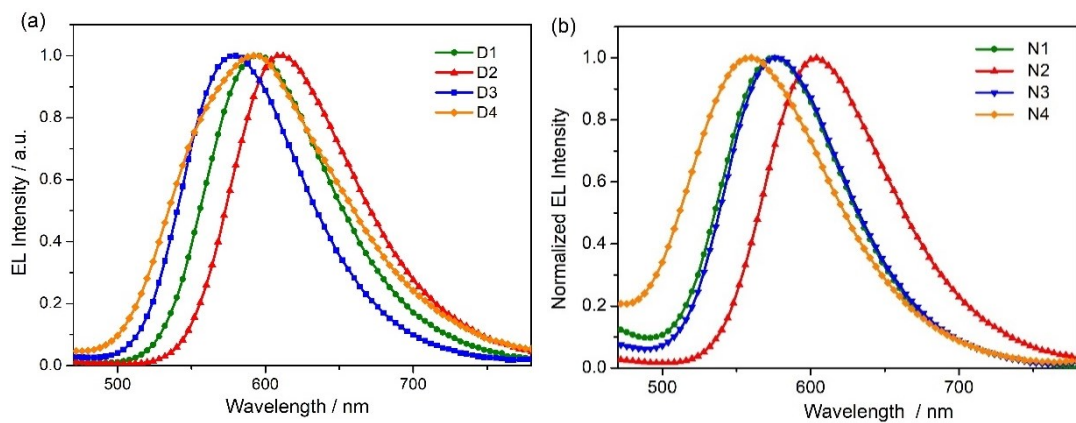
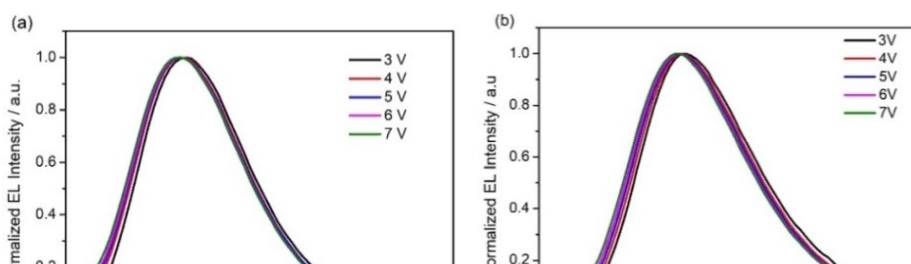
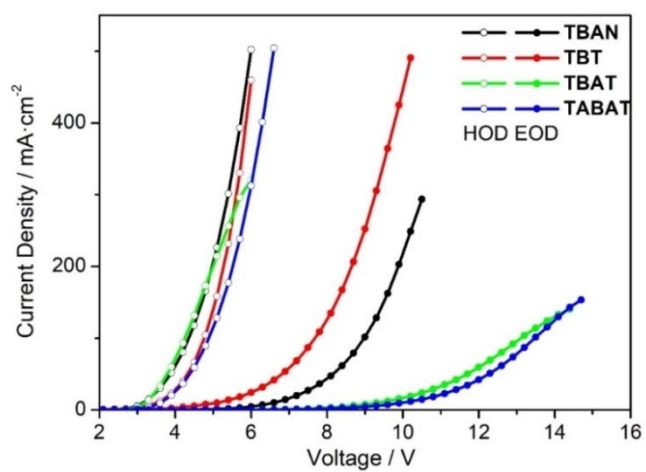


Fig. S11 the EL spectra of doped devices (a) and non-doped devices (b)





**Fig. S13**  $J$ - $V$  curves of all single devices based TBAN, TBT, TBAT and TABAT

## References

- [1] X. Tang, Q. Bai, T. Shan, J. Li, Y. Gao, F. Liu, H. Liu, Q. Peng, B. Yang, F. Li, P. Lu, *Adv. Funct. Mater.* **2018**, 28, 1705813.
- [2] A. D. Becke, *Phys. Rev. A* **1988**, 38, 3098-3100.
- [3] C. Lee, W. Yang, R. G. Parr, *Phys. Rev. B* 1988, 37, 785-789.